Chemical Science

ROYAL SOCIETY OF CHEMISTRY

PERSPECTIVE

View Article Online
View Journal | View Issue

Cite this: *Chem. Sci.*, 2022, **13**, 8243

All publication charges for this article have been paid for by the Royal Society of Chemistry

Towards the practical application of Zn metal anodes for mild aqueous rechargeable Zn batteries†

Ning Dong, Fenglin Zhang and Huilin Pan *

Rechargeable aqueous Zn batteries have been widely investigated in recent years due to the merits of high safety and low cost. However inevitable dendrite growth, corrosion and hydrogen evolution of Zn anodes severely compromise the practical lifespan of rechargeable Zn batteries. Despite the encouraging improvements for Zn anodes reported in the literature, the comprehensive understanding of Zn anodes under practical conditions is still often neglected. In this article, we focus on the "less-discussed" but critically important points for rechargeable aqueous Zn batteries, including revisit of the relationship between the coulombic efficiency and lifespan of Zn anodes, the rational control of the pH environment in the vicinity of Zn anodes, the design of appropriate aqueous separators and the relevant estimation of practical energy density for aqueous Zn batteries. It concludes that energy density of 60–80 W h kg^{-1} for aqueous Zn batteries should be realistic in practice with appropriate cell design. We also propose practical technical recommendations for the rational development of aqueous Zn batteries based on research experience from the community and our group. We hope this article offers readers more practical insights into the future development of aqueous Zn batteries as competitive technology for practical use.

Received 30th March 2022
Accepted 9th June 2022

DOI: 10.1039/d2sc01818g

rsc.li/chemical-science

1. Introduction

Electrochemical energy storage approaches such as commercial Li-ion batteries are highly attractive due to their high flexibility and high energy densities.[1] However, the limited resources of Li on the earth and the safety hazards of flammable organic electrolytes urge scientists to seek alternative low-cost and highly safe solutions for future large-scale energy storage. Recently, rechargeable aqueous Zn batteries using Zn metal as the anode have been revisited as a potential solution for grid energy storage due to the advantages of non-flammability, environmental benignity, low cost, *etc.*[2,3] Unlike most metals including Li, Na, K, Mg, Al, *etc.*, Zn metal can be directly applied as the anode for aqueous batteries and also exhibits a high theoretical capacity of 819 mA h g^{-1}, superior volumetric capacity of 5854 mA h cm^{-3} and low redox potential of −0.762 V *vs.* the standard hydrogen electrode. Owing to the insensitivity to oxygen and humid atmospheres, aqueous Zn-based batteries can be assembled under an air atmosphere without additional cost arising from harsh water-free and oxygen-free environments.[4]

Nevertheless, Zn metal anodes suffer from significant challenges, *i.e.*, dendrite growth, low reversibility, significant volume change and the hydrogen evolution reaction (HER) during continuous Zn plating and stripping processes. The intrinsic potholes and roughness of Zn foil result in uneven active sites and heterogeneous Zn^{2+} flux and then influence the Zn deposition morphology. In mildly acidic electrolytes, dendrite formation is alleviated compared with alkaline media but is still inevitable particularly at large current density and areal capacity, which may pierce the separator and cause short-circuit inside the batteries.[5] Dendrite and volume variation are the general issues for many metal anodes in rechargeable batteries, while some situations are specific to Zn anodes in aqueous systems. The HER is thermodynamically prior to Zn^{2+} deposition in mildly acidic aqueous electrolytes, leading to low coulombic efficiency (CE), consumption of aqueous electrolytes, buildup of internal cell pressure and thus increase of cell impedance. H_2 generation may also bring about local accumulation of OH^- and further generate an insulating hydroxide-Zn salt on the surface of Zn anodes, increasing the polarization voltages and degrading the battery performance.[6]

The instability of Zn anodes has been regarded as the most vital challenge and the bottleneck for the practical applications of Zn batteries.[7] A variety of approaches have been proposed to address the key challenges of Zn anodes, certain of which are based on the experience and knowledge for the development of rechargeable Li metal anodes.[8–10] Several review articles have

Department of Chemistry, Zhejiang University, Hangzhou, 310027, China. E-mail: panhuilin@zju.edu.cn

† Electronic supplementary information (ESI) available. See https://doi.org/10.1039/d2sc01818g

been presented on the topic of Zn anodes for rechargeable Zn batteries very recently,[11–15] which well summarized the development of new electrolytes, additives, electrode structures, surface modifications, alloy anodes, *etc.* The CE of Zn anodes has been increased to 99.9%,[16] and the cycling stability of Zn anodes has been extended to 10 000 cycles.[17] Undoubtedly, these studies provide valuable insights into the development of high-performance Zn anodes. Nevertheless, several remaining underlying issues lack good clarification, which largely hinders the practical applications of rechargeable Zn batteries as a viable solution for energy storage. In this perspective article, we will focus on discussing the "less-discussed" topics for Zn anodes, including revisiting the rational measurements of the CE and cycle life for Zn anodes, estimating the achievable energy density of aqueous Zn batteries, regulating the interfacial pH environment and designing advanced Zn alloy anodes and novel separators, all of which are crucial to develop high-performance aqueous Zn batteries in practice. We try to present readers a practical angle to look at the development of rechargeable Zn anodes, understand the underlying situations and scientific challenges for Zn metal batteries, and seek practical directions for the development of rechargeable Zn batteries. This work will also be of broad interest to the development of high-energy rechargeable batteries using metal-based anodes such as Li metal batteries. The main topics will be discussed in the following parts.

1.1. Revisit of the coulombic efficiency and cycle life of Zn anodes

The CE of Zn anodes can be defined as the ratio of the charge capacity to the discharge capacity of the electrode in a cell, which has been widely used as a quantitative indicator for the reversibility and lifespan of Zn anodes in the literature.[18] Like any other rechargeable metal batteries, the rational understanding and reasonable measurement methods of CE are of great importance to evaluate different modification strategies effectively and fairly. Several researchers have raised concerns regarding the accurate measurement of CE for rechargeable Zn batteries in recent years,[19,20] while a clear understanding of CE for Zn anodes is still lacking. The CE of Zn anodes is basically influenced by three types of irreversible reactions: (1) the HER that occurs during Zn plating contributes to apparent discharge capacity for Zn anodes but it is irreversible for the following Zn stripping process, resulting in obviously low CE; (2) the parasitic chemical and electrochemical reactions between Zn metal and aqueous electrolytes also lead to irreversible capacity for reduced CE; (3) the encapsulated Zn metal by insulating by-products is kinetically inactive, while the "dead Zn" might be occasionally resumed during repeated Zn deposition–dissolution processes.[21–23]

The above irreversible reactions on Zn anodes are strongly correlated with the test conditions of the batteries, which vary greatly from study to study even using the same electrolytes. Zn||Cu and Zn||Ti half cells are the most common and convenient approaches to measure the CE of Zn anodes, which contain Zn counter electrode as the Zn reservoir and Cu/Ti as working electrodes. Technically, the measurement of CE is influenced by various factors including the utilization of the Zn counter electrode and the applied current densities.[24] High utilization of the Zn counter electrode will affect the measurement of CE values (on the working electrode), which may be attributed to the influenced electrolyte environment and actual cut-off voltage during Zn stripping induced by the non-negligible parasitic reactions on the counter Zn electrode. The depth of discharge (DOD) of the Zn electrode is reasonably lower than 20% for appropriate evaluation of CE (Fig. 1a). Besides, for a given areal deposition capacity of Zn on the Cu/Ti working electrodes, a higher current density could lead to apparently higher CE values due to the reduced time for the parasitic reactions (Fig. 1b). It's important to evaluate the CE of Zn anodes under different current densities for comprehensive understanding of the reversibility of Zn anodes. But the high CE values under a large current density may be misleading for the thermodynamic stability and high reversibility of Zn batteries under practical cycling conditions. Furthermore, the type of current collector will also affect the CE of Zn electrodes by influencing the deposition morphology of Zn metal (Fig. 1c).

Apart from the external factors such as current density, Zn utilization *etc.*, electrolytes are the intrinsic reason for the reversibility of Zn anodes.[25] $ZnSO_4$, $Zn(TFSI)_2$ and $Zn(TfO)_2$ are the mostly studied Zn salts in aqueous electrolytes for Zn-based batteries. Without special modification, the electrolytes with $ZnSO_4$ salt exhibit significantly higher CE (~99–99.5% in the 20^{th} cycle) than $Zn(TFSI)_2$ (~70–90%) and $Zn(TfO)_2$ (~65–91%) salts (Fig. 1d–f). This is closely related to the different deposition morphologies of Zn in these electrolytes (Fig. S1†). The CE in $ZnSO_4$ aqueous electrolytes show no obvious correlation with the salt concentration, while the CE in aqueous electrolytes with both $Zn(TFSI)_2$ and $Zn(TfO)_2$ salts strongly correlates with the salt concentrations. Interestingly, the CE values do not exhibit a linear dependence with increased salt concentration of $Zn(TFSI)_2$ and $Zn(TfO)_2$ electrolytes as shown in Fig. 1e and f, and the CE values deteriorate much faster in aqueous electrolytes with an organic Zn salt than $ZnSO_4$-based aqueous electrolytes. These results suggest that $TFSI^-$ and TfO^- based organic Zn salts are intensively involved in the parasitic reactions on Zn anodes, and the decomposition of such electrolytes may be unable to appropriately protect Zn anodes from continuous side reactions during Zn deposition–dissolution, leading to fast decay of the CE during cycling (Table S4†).

Fig. 1g summarizes the reported CE values of >99% for different types of aqueous electrolytes with further modification such as adding additives, co-solvents and co-salts.[26–28] The detailed electrolytes and test conditions for CE values are listed in Table S1.† It is not rare to reach a CE of Zn anodes of >99.5% after certain cycles; however, achieving >99.9% CE is still a challenge for aqueous Zn batteries. Few studies with reported CE of Zn anodes more than 99.9% still require long-term cycling to reach high values.[16,29] It is critically important to reach >99.9% or even 99.99% CE after initial cycles like graphite anodes in Li-ion batteries. Otherwise, substantial active Zn will be lost during long-term cycling periods, and Zn anodes still fail

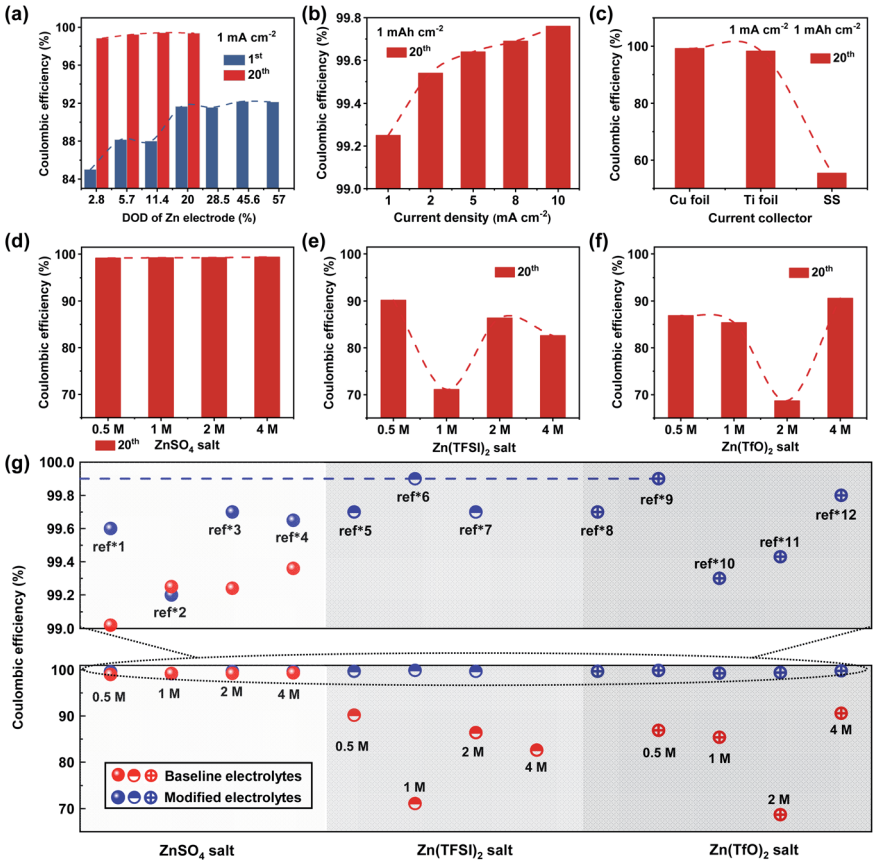

Fig. 1 Comparison of the coulombic efficiency of Zn anodes in the 1st and 20th cycles in Zn||Cu (Ti or stainless steel) cells under different test conditions. (a) Different DODs of Zn counter electrodes in a 1 M $ZnSO_4$ electrolyte at 1 mA cm^{-2} (correspond to an areal capacity of 0.5, 1, 2, 3.5, 5, 8 and 10 mA h cm^{-2} respectively); (b) different current densities in a 1 M $ZnSO_4$ electrolyte at 1 mA h cm^{-2}; (c) different current collectors in a 1 M $ZnSO_4$ electrolyte at 1 mA cm^{-2} and 1 mA h cm^{-2}, and different salt concentrations in aqueous electrolytes of (d) $ZnSO_4$, (e) $Zn(TFSI)_2$ and (f) $Zn(TfO)_2$ in Zn||Cu cells at 1 mA cm^{-2} and 1 mA h cm^{-2}. (g) Summary of published CE values of >99% from the literature in different Zn salt aqueous electrolytes under different test conditions (blue circles, the "ref*" represents the references in the ESI,† and the detailed test conditions of these references are described in Table S1†), and the baseline CE values (red circles) are from (d–f). Note that all experimental data in (a–f) and the baseline electrolytes in (g) are re-evaluated with 30 μm Zn counter electrodes in Zn||Cu cells, and the detailed experimental results of CE are listed in Tables S4 and S5.†

to meet the requirement for long-lasting rechargeable Zn batteries in practice.

In addition, it could be found that $ZnSO_4$-based aqueous electrolytes show no obvious enhancement in CE values after different modification methods, while $Zn(TFSI)_2$ and $Zn(TfO)_2$ based aqueous electrolytes exhibit remarkable enhancement for CE. This is likely because organic salts containing F^- are more prone to generate useful and controllable SEI layer components with the addition of functional additives and co-salts or solvents.[29] Nevertheless, a quantified understanding of the electrolyte decomposition pathway and the mechanism for the formation of a sustainable SEI layer in aqueous electrolytes with organic Zn salts is far from being well-understood in aqueous Zn batteries. The charge transport kinetics in the aqueous-based SEI layer and its dynamic evolution from both microcosmic and macroscopic viewpoints are highly required to be well understood to develop highly reversible and long-lasting Zn anodes in future study.

Appropriate evaluation of CE could be highly relevant to the lifespan of Zn anodes. Among the aqueous electrolytes with different Zn salts, $ZnSO_4$-based aqueous electrolytes with the highest CE present 2–5 times longer lifespan than $Zn(TFSI)_2$ and $Zn(TfO)_2$ based aqueous electrolytes (Fig. 2a). With modifications for different types of aqueous electrolytes, the reported cycle life could be improved to 3000 hours for Zn-based half cells[30] and 6000 hours for Zn||Zn symmetric cells[29] in the literature report. It should be noted that the baseline and the improvement in cycle life for Zn anodes vary significantly from study to study, even with the same electrolytes and testing protocol.[13,31] Shallow cycling of Zn electrodes with an abundant electrolyte delivers an arbitrary long cycle life even with low CE values because the Zn reservoir can continuously provide active Zn (Table S2†).[18] Meanwhile the continuous loss of active Zn will cause quick capacity attenuation and limited lifespan in a practical Zn battery without extra Zn resources. It is found that the lifespan of Zn electrodes in Zn||Cu cells with $ZnSO_4$ aqueous electrolytes is 1000 hours on average under a current density of 1 mA cm^{-2}, with a Zn utilization of 0.68%. When increasing the Zn utilization to 2.9%, the cycle life of the Zn counter electrode exhibits exponential decay for only 190 hours on average. When

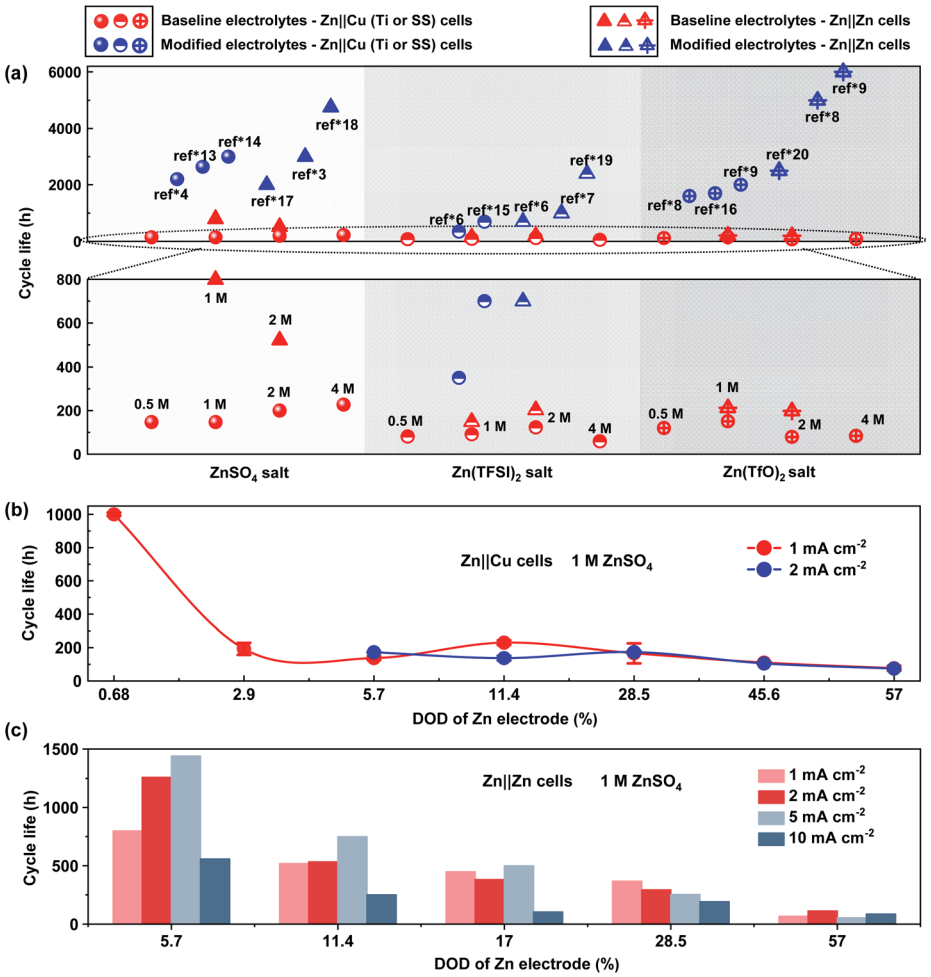

Fig. 2 Cycle life curves of Zn anodes in Zn||Cu (Ti or SS) half cells and Zn||Zn symmetric cells under different test conditions. (a) Comparison between the baseline $ZnSO_4$, $Zn(TFSI)_2$, and $Zn(TfO)_2$ based aqueous electrolytes with different salt concentrations (red circles: Zn||Cu cells; red triangles: Zn||Zn cells; 1 mA cm^{-2} and 1 mA h cm^{-2}) and modified aqueous electrolytes in published reports under different test conditions (blue circles: Zn||Cu cells; blue triangles: Zn||Zn cells; the "ref*" represents the references in the ESI,† and the detailed test conditions of these references are described in Tables S2 and S3†); (b) different DODs of Zn anodes with a 1 M $ZnSO_4$ electrolyte at 1 mA cm^{-2} and 2 mA cm^{-2} in Zn||Cu half cells; (c) different DODs of Zn anodes with a 1 M $ZnSO_4$ electrolyte at different current densities in Zn||Zn cells. Note that the cycle life of baseline electrolytes in Fig. 2a and the experimental data in Fig. 2b and c are re-evaluated with 30 μm and 250 μm Zn electrodes, and the detailed experimental results are listed in Table S4–S6.†

further increasing the Zn utilization to 60%, the cycle life of Zn||Cu cells changes slightly and decreases along with increased DOD under both 1 mA cm^{-2} and 2 mA cm^{-2} (Fig. 2b). The results suggest that the measurement of cycle life may be inaccurate with the DOD of Zn electrodes lower than 1% in Zn||Cu cells. Zn||Zn symmetric cells exhibit a longer cycle life than Zn||Cu cells and present basically similar attenuation in cycle life when increasing the utilization of Zn (Fig. 2c). Under a given utilization of Zn, the cycle life of symmetric cells and morphology of Zn deposition strongly correlate with the applied current densities. The Zn electrode in the Zn||Zn cell (Zn utilization of 5.7%) with a $ZnSO_4$ electrolyte delivers the longest cycle life of more than 1400 hours under a current density of 5 mA cm^{-2}, which is almost twice the life under 1 mA cm^{-2}. As shown in Fig. S2,† small current densities favor the growth of a large Zn deposition morphology with a reduced specific surface area, while enabling abundant time to generate by-products as well. Large current densities benefit a smaller and more uniform Zn deposition morphology due to high overpotential.[32] The large current densities might also cause Zn dendrite growth due to the limited diffusion of Zn^{2+}.[33] Therefore, the dependence of cycle life on the current density is typically very complicated in practice, which depends on the specific situations of Zn deposition, such as interfacial Zn^{2+} transport, electroconvection, *etc.*

1.2. pH environment for Zn anodes

The thermodynamic voltage for the deposition–dissolution of Zn anodes is overlapped with the voltage range for the HER, both of which are highly correlated with the pH environment of the electrolyte solutions.[34,35] Regulating the pH of electrolytes can significantly influence the occurrence of the HER. Meanwhile, the H_2 generation at Zn anodes also influences the local pH environment of electrolytes in turn.[36] As depicted in Fig. 3a,

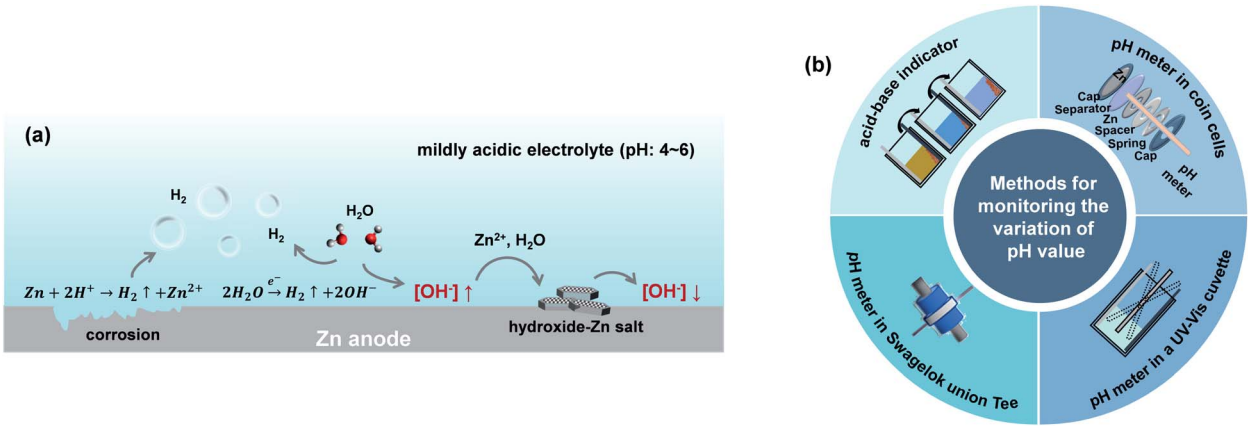

Fig. 3 (a) Schematic illustrations of the reactions under an unstable pH environment at the vicinity of Zn anodes. (b) *In situ* pH monitoring methods for aqueous Zn batteries.

OH^- accumulates locally when the HER occurs at the Zn anode, thus leading to the precipitation of an insulating hydroxide-Zn salt on the surface of the Zn anode. The inert byproducts can cause an inhomogeneous anode surface, resulting in uneven Zn deposition–dissolution and increased cell resistance. The influence of pH values in $ZnSO_4$ electrolytes on the Zn deposition morphology is also investigated in Fig. S3.† A few recent studies have been proposed to stabilize the pH values at the interface between the Zn anode and electrolyte such as electrolyte modification with pH buffer to regulate H^+/OH^- concentration,[37,38] constructing ion-selective coating layers to isolate the Zn anode from the electrolyte.[39] By stabilizing the pH values at the interface between the Zn anode and electrolyte, the accumulation of OH^- at the vicinity of the Zn anode can be efficiently suppressed and thus enables sustainably fast reaction kinetics on the Zn anode, suppressing the side reactions and precipitation of insoluble by-products on the Zn anode.[40]

Besides, developing *in situ* pH monitoring techniques for aqueous Zn batteries could provide constructive guidelines to stabilize the Zn–electrolyte interfacial environment for stable Zn deposition. Several approaches for *in situ* monitoring pH values have been developed, including the utilization of an acid–base indicator to visualize the local color change,[41] applying pH meters in a Swagelok union Tee[42] or electrochemical cells in a UV-Vis cuvette[41] or drilled coin cells[43] (Fig. 3b). But it is still challenging to exhibit high spatial resolution of the pH environment and its evolution near the surface of Zn anodes for precise control of Zn deposition–dissolution. A future combination of molecular acid–base indicators with a certain *operando* microscopy technique such as micro-Raman or atomic force microscopy could be helpful to study the electrochemical interfacial process from a microscopic viewpoint.[44,45]

1.3. Introduction of Zn-based alloy anodes

Introducing a Zn-based alloy could be a viable approach to improve the corrosion resistance of Zn anodes and enhance the uniformity of Zn deposition for practical aqueous Zn-based

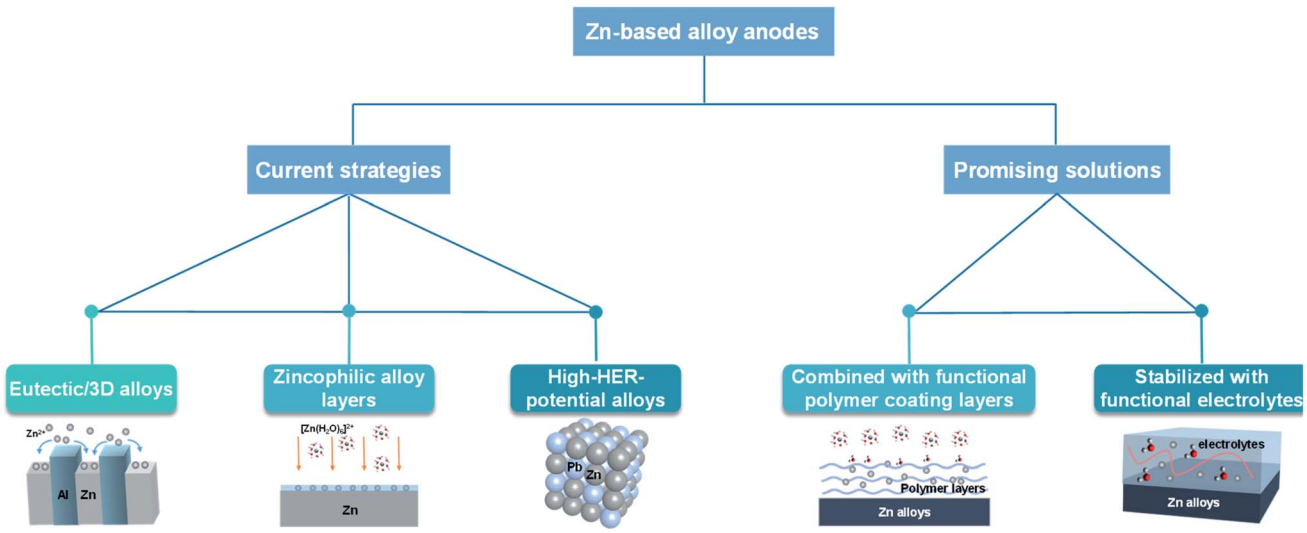

Fig. 4 The development of Zn-based alloy anodes for aqueous Zn batteries.

batteries.[46,47] Currently, the progress on Zn-based alloy anodes is lagging far behind the development of advanced electrolytes and electrode structures.[48] Researchers have tried to design eutectic alloyed anodes[49] or 3D Zn alloy anodes[50] to regulate homogeneous Zn deposition, use zincophilic alloy layers[51] to decrease the nucleation barrier for Zn deposition or provide a larger overpotential for the HER[52] (Fig. 4). During practical cycling, Zn alloy anodes inevitably exhibit continuous change in structures and compositions during repeated Zn deposition and dissolution processes. This might make the initial design of Zn alloy anodes quickly fail during cycling especially under high utilization of Zn anodes. Detailed investigation on the dynamic evolution of the morphology, composition, and distribution of alloying elements in Zn-based alloy electrodes and approaches of stabilizing Zn alloy anodes during repeated cycling should be carefully investigated in the future. Our group has recently proposed a synergistic optimization strategy of a porous metal coating layer combined with a functional polymer gel electrolyte layer for greatly improved structural stability of Zn alloy anodes. The functional polymer gel electrolyte layer enhances homogeneous Zn^{2+} distribution in the vicinity of Zn anodes and stabilizes the composite alloy anodes under high utilization of Zn. Similarly, Zhang *et al.*[53] also proposed a synergistic method that combined the Cu–Zn solid solution interface on a copper mesh skeleton with good Zn affinity and a polyacrylamide electrolyte additive to modify the Zn anode. The combination of a stable three-dimensional alloy electrode and easily available electrolyte additive could be an effective strategy to promote the Zn nucleation, which provides robust structural support and uniform Zn deposition simultaneously. Therefore, it could be important to develop synergistic combination of different approaches to further enhance the reaction uniformity of Zn electrodes and retain the structural stability of Zn alloy anodes (Fig. 4).

1.4. Development of appropriate separators

Besides the active components in a cell, the study of inactive components, such as the separator, is often neglected.[54] The separator is the essential part in a cell that separates the cathode and anode, provides sufficient ionic conductivity and appropriate mechanical strength to avoid short-circuit by dendrite growth.[55,56] Unlike non-aqueous batteries, excellent hydrophilicity of the separator towards aqueous electrolytes is crucial for aqueous batteries.[57] Commercial polyolefin separators used in Li-ion batteries are usually not appropriate for aqueous Zn batteries owing to the poor wettability. Glass fiber and cellulose membranes exhibit superior hydrophilicity and large pores, which are widely employed as separators for aqueous Zn batteries in the current study.[58,59] However, the inferior mechanical properties of cellulose and the excessive thickness of glass fiber limit their practical application, and the large pores in the separators could induce heterogenous Zn deposition. The modification of ordinary glass fiber or cellulose separators by surface coating or functional decoration has been reported to be effective for improved Zn deposition.[60,61] Besides, syntheses of new aqueous separators with a cross-linked hydrophilic polymer framework such as polyacrylonitrile (PAN),[62] polyacrylic acid (PAA),[63] and Nafion[64] have also been proposed for a tailored Zn^{2+} diffusion pathway and thus regulating smooth Zn deposition. Nevertheless, it still needs further clarification and deeper understanding on how to rationally regulate the Zn^{2+} flux and diffusion kinetics by appropriate design for the pore structures of the separators. It is noted that the pore structures (*i.e.*, diameter, shape, tortuosity, *etc.*) and mechanical strength of separators should be well balanced when designing new separators.[65] Furthermore, the manufacturing costs should also be considered for the practical application of aqueous separators.

1.5. Energy density of aqueous Zn batteries

Owing to the high theoretical specific capacity of Zn anodes and multi-charge intercalation chemistry of Zn^{2+}, mildly acidic aqueous Zn batteries are expected to deliver high gravimetric energy density and have attracted surging interest in the research community.[66–68] In practice, the achievable energy density of aqueous Zn batteries should be carefully considered for the use of many inactive components (carbon additives, current collectors, separators, cell package, *etc.*) and extra Zn metal anodes.[12,69] However, a rational evaluation of energy density for aqueous Zn batteries is lacking in the literature. We consider several important parameters to roughly estimate the achievable gravimetric energy density of different battery chemistries from the practical perspective according to the following eqn (1) (the detailed calculation process of eqn (1) (ref. 70) is presented in the ESI†):

$$E = k\frac{U}{\frac{1}{C_+}+\frac{R}{C_-}} \quad (1)$$

where E is the estimated gravimetric energy density; C_+ and C_- are the specific capacity of the cathode material and Zn anode respectively; U is the average voltage of the battery; k is the mass fraction of active cathode and anode materials in the cell; R is the cell balance (N/P ratio, the ratio of negative electrode capacity to positive electrode capacity).

In Fig. 5, we show the estimation of the gravimetric energy density for the widely studied cathode materials of MnO_2 and V_2O_5 as a function of different k values and N/P ratios. Different charge storage mechanisms for the cathode materials are also taken into consideration. The MnO_2 cathode could deliver a theoretical capacity of ~308 mA h g^{-1} corresponding to one-electron transfer with an average voltage of ~1.3 V *vs.* Zn^{2+}/Zn. A theoretical capacity of 819 mA h g^{-1} is used for the Zn metal anode. With a 0.5 Zn^{2+} intercalation mechanism (eqn (2)), the energy density of Zn‖MnO_2 aqueous batteries is up to 175 W h kg^{-1} when $k = 0.6$ and N/P ratio = 1 are used as shown in Fig. 5a, which is even competitive to certain nonaqueous Li-ion batteries (*e.g.*, the commercial $LiFePO_4$ cathode).[71,72] However, extra Zn metal is typically required in rechargeable metal batteries for a decent cycle life, exhibiting N/P ratios larger than 1. It could be found that the estimated achievable energy density of Zn‖MnO_2 batteries decreases to 113 W h kg^{-1}

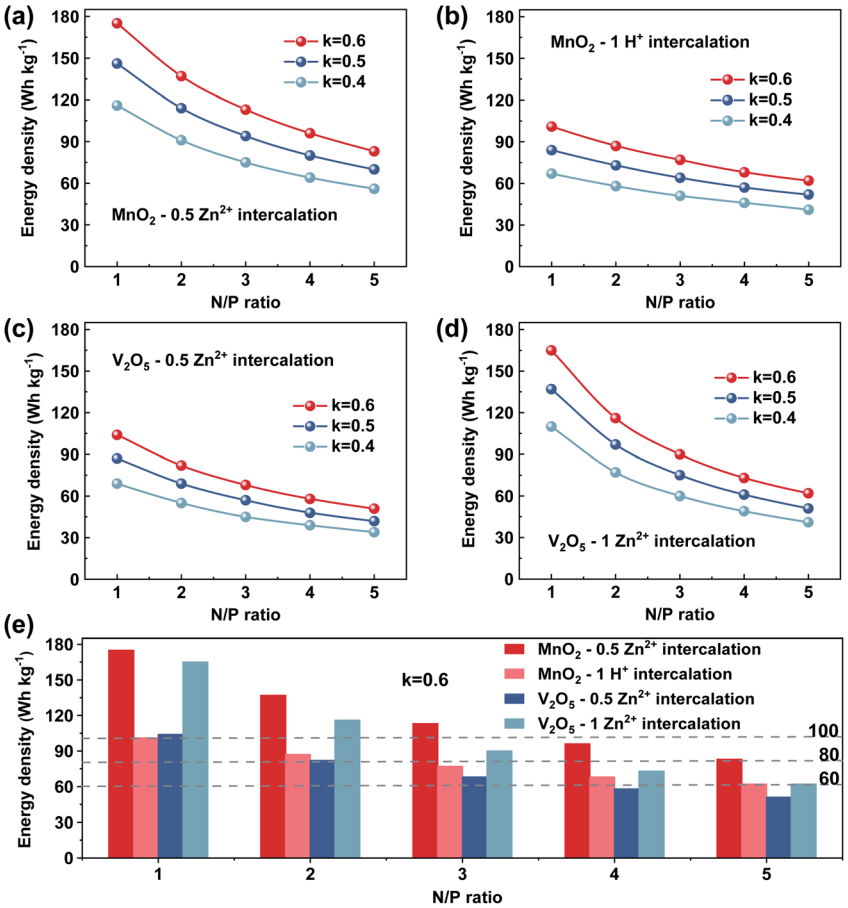

Fig. 5 Calculated gravimetric energy densities of different aqueous Zn battery chemistries *versus* N/P ratios and k values. (a) MnO_2 cathode with 0.5 Zn^{2+} intercalation reaction. (b) MnO_2 cathode with 1 H^+ intercalation reaction. (c) V_2O_5 cathode with 0.5 Zn^{2+} intercalation reaction. (d) V_2O_5 cathode with 1 Zn^{2+} intercalation reaction paired with a Zn metal anode. (e) Comparison of the gravimetric energy densities of the above battery chemistries *versus* different N/P ratios with $k = 0.6$.

and 83 W h kg^{-1} for N/P values of 3 and 5, respectively (Fig. 5a). A too large N/P ratio will greatly compromise the achievable energy density of aqueous Zn batteries. N/P ratios in a range of 2–5 could be reasonable considering both cycle life and energy density in practice. It is noted that $k = 0.5$–0.6 is the empirical value for commercial Li-ion batteries when estimating the practical energy density.[70,73] Aqueous Zn batteries may adopt a similar or slightly lower k value due to more electrolyte usage. The estimations for the energy density of Zn‖MnO_2 batteries are also presented under the conditions of $k = 0.5$ and 0.4 in Fig. 5a. In practical operation of Zn‖MnO_2 batteries, the H^+ interaction and the corresponding formation of hydroxide Zn salt precipitate (eqn (3)) could occur on the MnO_2 cathode, which would further reduce the achievable energy density due to the participation of aqueous electrolytes during the charge storage process.[74,75] When only considering the 1 H^+ insertion reaction as described in eqn (3), Zn‖MnO_2 could only deliver 101, 77 and 62 W h kg^{-1} at the N/P ratios of 1, 3 and 5, respectively (Fig. 5b, $k = 0.6$, and $x = 4$).

$$MnO_2 + \frac{1}{2}Zn^{2+} + e^- \leftrightarrow Zn_{\frac{1}{2}}MnO_2 \quad (2)$$

$$MnO_2 + H^+ + e^- + \frac{1}{6}ZnSO_4 + \frac{1}{2}Zn^{2+} + OH^- + \frac{x}{6}H_2O \leftrightarrow MnOOH + \frac{1}{6}ZnSO_4[Zn(OH_2)_3 \cdot xH_2O] \quad (3)$$

Compared with MnO_2 cathodes, V_2O_5 cathodes typically present a simpler charge storage mechanism with Zn^{2+} intercalation. When considering 0.5 Zn^{2+} interaction, V_2O_5 shows a theoretical capacity of 294 mA h g^{-1} and an average voltage of ~0.8 V *vs.* Zn^{2+}/Zn. The energy density of Zn‖V_2O_5 batteries could only reach 104 W h kg^{-1} at a N/P ratio of 1 and k value of 0.6 (Fig. 5c). A larger N/P value is needed for reasonable cycle life in practical applications. When $k = 0.6$ and N/P ratio = 3, the energy density of Zn‖V_2O_5 batteries could only reach 68 W h kg^{-1} as shown in Fig. 5c (red color curve). Besides, V_2O_5 cathodes have been reported to deliver a much higher capacity than 294 mA h g^{-1}, suggesting that more than 0.5 Zn^{2+} could be inserted into V_2O_5 cathodes.[76,77] When considering 1 Zn^{2+} interaction (589 mA h g^{-1}), the Zn‖V_2O_5 battery could deliver improved energy density as shown in Fig. 5d. For example, 90 W h kg^{-1} could be potentially achieved when $k = 0.6$ and N/P ratio = 3 are used (red color curve in Fig. 5d).

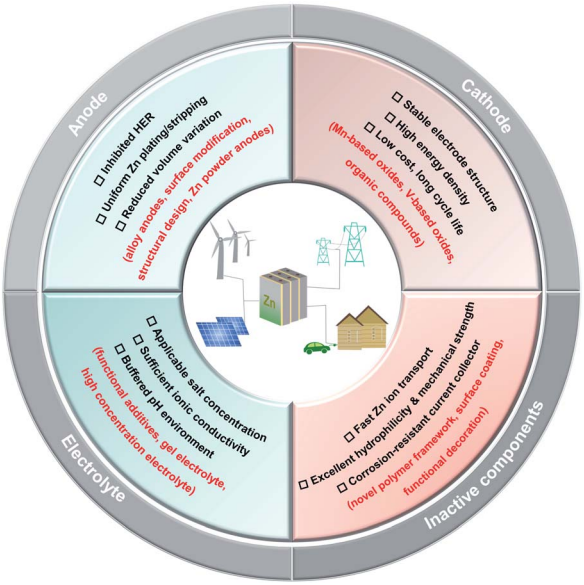

Fig. 6 Prospective strategies towards practical aqueous Zn batteries.

Based on the above discussion, aqueous Zn batteries could potentially achieve an energy density of 60 W h kg^{-1} under the conditions of $k = 0.6$ and N/P ratio = 3 either with MnO_2 or V_2O_5 cathodes (Fig. 5e). An energy density of 80 W h kg^{-1} for aqueous Zn batteries could be achieved with appropriate design, but 100 W h kg^{-1} could be very hard with a relevant cycle life. Manganese oxide cathodes could present higher energy density and lower cost than vanadium oxide cathodes as shown in Fig. 5e. Recently, a $2e^-$ charge storage mechanism (*i.e.*, 616 mA h g^{-1}) in a MnO_2 cathode has also been reported in alkaline Zn||MnO_2 batteries[78,79] and Mn^{2+}/MnO_2 cathodes,[80,81] which could further enhance the achievable energy density when applied with appropriate cell configurations. Nevertheless, the slightly sluggish reaction kinetics in MnO_2 cathodes and the dynamic change of the solid–liquid interface and structural stability of MnO_2 cathodes should be further enhanced to realize a long lifespan for practical use in the future.

2. Conclusions

In this article, we revisit the rational measurements of the CE and cycle life of Zn anodes when developing new approaches for aqueous Zn batteries. The rational control of the pH environment in an aqueous electrolyte and the development of *in situ* characterization methods, the design of advanced Zn alloy anodes and the hydrophilic, robust separators are discussed to provide useful insights to make up for the "less-developed" but important aspects for rechargeable aqueous Zn batteries. We also provide a simple and effective method to rationally estimate the achievable energy density of aqueous Zn batteries with different battery chemistries. The prospective strategies and future research emphasis are also discussed to promote aqueous Zn batteries to be a real competitive technology for practical use, mainly including inhibiting the HER, dendrite growth and volume expansion for Zn anodes, developing highly stable and low-cost cathodes, matching appropriate electrolyte systems with enhanced electrochemical properties and optimizing the compatibility and stability of inactive components for aqueous Zn batteries (Fig. 6).

Data availability

Extended data supporting this article are available in the ESI.†

Author contributions

H. P. conceived and supervised the research. N. D. and F. Z. performed the experiment and analysed the experimental data. N. D. and H. P. wrote and revised the paper. All authors contributed to the discussions.

Conflicts of interest

There are no conflicts to declare.

Acknowledgements

This work was supported by the National Natural Science Foundation of China (Grant No. 22179117 and U21A2075), Startup Foundation for Hundred-Talent Program of Zhejiang University and program of State Key Laboratory of Clean Energy Utilization at Zhejiang (ZJUCEU2020005). The kind help from Professor Hong Li at the Institute of Physics, Chinese Academy of Sciences for valuable insights and suggestions is also acknowledged.

Notes and references

1 M. Li, J. Lu, Z. Chen and K. Amine, *Adv. Mater.*, 2018, **30**, e1800561.
2 M. Yan, H. Ni and H. Pan, *Adv. Energy Sustainability Res.*, 2020, 2000026.
3 J. Song, K. Xu, N. Liu, D. Reed and X. Li, *Mater. Today*, 2021, **45**, 191–212.
4 T. Wang, C. Li, X. Xie, B. Lu, Z. He, S. Liang and J. Zhou, *ACS Nano*, 2020, **14**, 16321–16347.
5 J. Shin, J. Lee, Y. Park and J. W. Choi, *Chem. Sci.*, 2020, **11**, 2028–2044.
6 C. Xie, Y. Li, Q. Wang, D. Sun, Y. Tang and H. Wang, *Carbon Energy*, 2020, **2**, 540–560.
7 Z. Yi, G. Chen, F. Hou, L. Wang and J. Liang, *Adv. Energy Mater.*, 2020, 2003065.
8 M. Cui, Y. Xiao, L. Kang, W. Du, Y. Gao, X. Sun, Y. Zhou, X. Li, H. Li, F. Jiang and C. Zhi, *ACS Appl. Energy Mater.*, 2019, **2**, 6490.
9 Y. Zhang, J. D. Howe, S. Ben-Yoseph, Y. Wu and N. Liu, *ACS Energy Lett.*, 2021, **6**, 404.
10 Y. An, Y. Tian, K. Zhang, Y. Liu, C. Liu, S. Xiong, J. Feng and Y. Qian, *Adv. Funct. Mater.*, 2021, 2101886.
11 C. Li, X. Xie, S. Liang and J. Zhou, *Energy Environ. Mater.*, 2020, **3**, 146–159.

12 F. Wan, X. Zhou, Y. Lu, Z. Niu and J. Chen, *ACS Energy Lett.*, 2020, **5**, 3569–3590.
13 G. Fang, J. Zhou, A. Pan and S. Liang, *ACS Energy Lett.*, 2018, **3**, 2480–2501.
14 D. Chao, W. Zhou, F. Xie, C. Ye, H. Li, M. Jaroniec and S. Z. Qiao, *Sci. Adv.*, 2020, **6**, eaba4098.
15 L. E. Blanc, D. Kundu and L. F. Nazar, *Joule*, 2020, **4**, 771–799.
16 L. Cao, D. Li, T. Deng, Q. Li and C. Wang, *Angew. Chem.*, 2020, **59**, 19292–19296.
17 J. Zheng, Q. Zhao, T. Tang, J. Yin, C. D. Quilty, G. D. Renderos, X. Liu, Y. Deng, L. Wang, D. C. Bock, C. Jaye, D. Zhang, E. S. Takeuchi, K. J. Takeuchi, A. C. Marschilok and L. A. Archer, *Science*, 2019, **366**, 645–648.
18 J. Xiao, Q. Li, Y. Bi, M. Cai, B. Dunn, T. Glossmann, J. Liu, T. Osaka, R. Sugiura, B. Wu, J. Yang, J.-G. Zhang and M. S. Whittingham, *Nat. Energy*, 2020, **5**, 561–568.
19 L. Ma, M. A. Schroeder, O. Borodin, T. P. Pollard, M. S. Ding, C. Wang and K. Xu, *Nat. Energy*, 2020, **5**, 743–749.
20 G. Zampardi and F. La Mantia, *Nat. Commun.*, 2022, **13**, 687.
21 C. Jin, T. Liu, O. Sheng, M. Li, T. Liu, Y. Yuan, J. Nai, Z. Ju, W. Zhang, Y. Liu, Y. Wang, Z. Lin, J. Lu and X. Tao, *Nat. Energy*, 2021, **6**, 378–387.
22 F. Liu, R. Xu, Y. Wu, D. T. Boyle, A. Yang, J. Xu, Y. Zhu, Y. Ye, Z. Yu, Z. Zhang, X. Xiao, W. Huang, H. Wang, H. Chen and Y. Cui, *Nature*, 2021, **600**, 659–663.
23 Y. Zhang, J. D. Howe, S. Ben-Yoseph, Y. Wu and N. Liu, *ACS Energy Lett.*, 2021, **6**, 404–412.
24 L. Ma, M. A. Schroeder, T. P. Pollard, O. Borodin, M. S. Ding, R. Sun, L. Cao, J. Ho, D. R. Baker, C. Wang and K. Xu, *Energy Environ. Mater.*, 2020, **3**, 516–521.
25 G. M. Hobold, J. Lopez, R. Guo, N. Minafra, A. Banerjee, Y. Shirley Meng, Y. Shao-Horn and B. M. Gallant, *Nat. Energy*, 2021, **6**, 951–960.
26 K. Guan, L. Tao, R. Yang, H. Zhang, N. Wang, H. Wan, J. Cui, J. Zhang, H. Wang and H. Wang, *Adv. Energy Mater.*, 2022, 2103557, DOI: **10.1002/aenm.202103557**.
27 H. Qiu, X. Du, J. Zhao, Y. Wang, J. Ju, Z. Chen, Z. Hu, D. Yan, X. Zhou and G. Cui, *Nat. Commun.*, 2019, **10**, 5374.
28 Y. Dong, L. Miao, G. Ma, S. Di, Y. Wang, L. Wang, J. Xu and N. Zhang, *Chem. Sci.*, 2021, **12**, 5843–5852.
29 L. Cao, D. Li, T. Pollard, T. Deng, B. Zhang, C. Yang, L. Chen, J. Vatamanu, E. Hu, M. J. Hourwitz, L. Ma, M. Ding, Q. Li, S. Hou, K. Gaskell, J. T. Fourkas, X. Q. Yang, K. Xu, O. Borodin and C. Wang, *Nat. Nanotechnol.*, 2021, **16**, 902–910.
30 Y. Jin, K. S. Han, Y. Shao, M. L. Sushko, J. Xiao, H. Pan and J. Liu, *Adv. Funct. Mater.*, 2020, **30**, 2003932.
31 C. Zhao, X. Wang, C. Shao, G. Li, J. Wang, D. Liu and X. Dong, *Sustainable Energy Fuels*, 2021, **5**, 332–350.
32 H. Glatz, E. Tervoort and D. Kundu, *ACS Appl. Mater. Interfaces*, 2020, **12**, 3522–3530.
33 J. Kasemchainan, S. Zekoll, D. Spencer Jolly, Z. Ning, G. O. Hartley, J. Marrow and P. G. Bruce, *Nat. Mater.*, 2019, **18**, 1105–1111.
34 J. Hao, X. Li, X. Zeng, D. Li, J. Mao and Z. Guo, *Energy Environ. Sci.*, 2020, **13**, 3917–3949.
35 L. Hu, P. Xiao, L. Xue, H. Li and T. Zhai, *EnergyChem*, 2021, **3**, 100052.
36 W. Du, E. H. Ang, Y. Yang, Y. Zhang, M. Ye and C. C. Li, *Energy Environ. Sci.*, 2020, **13**, 3330–3360.
37 D. Han, Z. Wang, H. Lu, H. Li, C. Cui, Z. Zhang, R. Sun, C. Geng, Q. Liang, X. Guo, Y. Mo, X. Zhi, F. Kang, Z. Weng and Q. H. Yang, *Adv. Energy Mater.*, 2022, 2102982.
38 M. Li, Z. Li, X. Wang, J. Meng, X. Liu, B.-k. Wu, C. Han and L. Mai, *Energy Environ. Sci.*, 2021, **14**, 3796–3839.
39 Y. Jiao, F. Li, X. Jin, Q. Lei, L. Li, L. Wang, T. Ye, E. He, J. Wang, H. Chen, J. Lu, R. Gao, Q. Li, C. Jiang, J. Li, G. He, M. Liao, H. Zhang, I. P. Parkin, H. Peng and Y. Zhang, *Adv. Funct. Mater.*, 2021, 2107652.
40 X. Zhao, X. Zhang, N. Dong, M. Yan, F. Zhang, K. Mochizuki and H. Pan, *Small*, 2022, e2200742.
41 C. F. Bischoff, O. S. Fitz, J. Burns, M. Bauer, H. Gentischer, K. P. Birke, H.-M. Henning and D. Biro, *J. Electrochem. Soc.*, 2020, **167**, 020545.
42 B. Lee, H. R. Seo, H. R. Lee, C. S. Yoon, J. H. Kim, K. Y. Chung, B. W. Cho and S. H. Oh, *ChemSusChem*, 2016, **9**, 2948–2956.
43 Q. Yang, L. Li, T. Hussain, D. Wang, L. Hui, Y. Guo, G. Liang, X. Li, Z. Chen, Z. Huang, Y. Li, Y. Xue, Z. Zuo, J. Qiu, Y. Li and C. Zhi, *Angew. Chem.*, 2022, **61**, e202112304.
44 W. Li, D. M. Lutz, L. Wang, K. J. Takeuchi, A. C. Marschilok and E. S. Takeuchi, *Joule*, 2021, **5**, 77–88.
45 Y. H. Wang, S. Zheng, W. M. Yang, R. Y. Zhou, Q. F. He, P. Radjenovic, J. C. Dong, S. Li, J. Zheng, Z. L. Yang, G. Attard, F. Pan, Z. Q. Tian and J. F. Li, *Nature*, 2021, **600**, 81–85.
46 G. Song, J. Y. Cheong, C. Kim, L. Luo, C. Hwang, S. Choi, J. Ryu, S. Kim, W. J. Song, H. K. Song, C. Wang, I. D. Kim and S. Park, *Nat. Commun.*, 2019, **10**, 2364.
47 Z. Cai, Y. Ou, B. Zhang, J. Wang, L. Fu, M. Wan, G. Li, W. Wang, L. Wang, J. Jiang, Z. W. Seh, E. Hu, X. Q. Yang, Y. Cui and Y. Sun, *J. Am. Chem. Soc.*, 2021, **143**, 3143–3152.
48 Q. Zhang, J. Luan, Y. Tang, X. Ji and H. Wang, *Angew. Chem.*, 2020, **59**, 13180–13191.
49 S. B. Wang, Q. Ran, R.-Q. Yao, H. Shi, Z. Wen, M. Zhao, X. Y. Lang and Q. Jiang, *Nat. Commun.*, 2020, **11**, 1634.
50 B. Liu, S. Wang, Z. Wang, H. Lei, Z. Chen and W. Mai, *Small*, 2020, **16**, e2001323.
51 P. Cao, J. Tang, A. Wei, Q. Bai, Q. Meng, S. Fan, H. Ye, Y. Zhou, X. Zhou and J. Yang, *ACS Appl. Mater. Interfaces*, 2021, **13**, 48855–48864.
52 C. Han, W. Li, H. K. Liu, S. Dou and J. Wang, *Nano Energy*, 2020, **74**, 104880.
53 Q. Zhang, J. Luan, L. Fu, S. Wu, Y. Tang, X. Ji and H. Wang, *Angew. Chem.*, 2019, **58**, 15841.
54 E. Foreman, W. Zakri, M. Hossein Sanatimoghaddam, A. Modjtahedi, S. Pathak, A. G. Kashkooli, N. G. Garafolo and S. Farhad, *Adv. Sustainable Syst.*, 2017, **1**, 1700061.
55 Q. Nian, T. Sun, S. Liu, H. Du, X. Ren and Z. Tao, *Chem. Eng. J.*, 2021, **423**, 130253.
56 H. He, H. Qin, J. Wu, X. Chen, R. Huang, F. Shen, Z. Wu, G. Chen, S. Yin and J. Liu, *Energy Storage Mater.*, 2021, **43**, 317.

57 K. K. Jana, S. J. Lue, A. Huang, J. F. Soesanto and K.-L. Tung, *ChemBioEng Rev.*, 2018, **5**, 346–371.
58 Y. Qin, P. Liu, Q. Zhang, Q. Wang, D. Sun, Y. Tang, Y. Ren and H. Wang, *Small*, 2020, **16**, e2003106.
59 H. Jia, Z. Wang, B. Tawiah, Y. Wang, C. Y. Chan, B. Fei and F. Pan, *Nano Energy*, 2020, **70**, 104523.
60 W. Zhou, M. Chen, Q. Tian, J. Chen, X. Xu and C. P. Wong, *Energy Storage Mater.*, 2022, **44**, 57–65.
61 Z. Hou, Y. Gao, H. Tan and B. Zhang, *Nat. Commun.*, 2021, **12**, 3083.
62 B. S. Lee, S. Cui, X. Xing, H. Liu, X. Yue, V. Petrova, H. D. Lim, R. Chen and P. Liu, *ACS Appl. Mater. Interfaces*, 2018, **10**, 38928–38935.
63 S. Huang, F. Wan, S. Bi, J. Zhu, Z. Niu and J. Chen, *Angew. Chem.*, 2019, **58**, 4313–4317.
64 B. Wu, Y. Wu, Z. Lu, J. Zhang, N. Han, Y. Wang, X.-m. Li, M. Lin and L. Zeng, *J. Mater. Chem. A*, 2021, **9**, 4734–4743.
65 W. Lu, C. Xie, H. Zhang and X. Li, *ChemSusChem*, 2018, **11**, 3996–4006.
66 Y. P. Deng, R. Liang, G. Jiang, Y. Jiang, A. Yu and Z. Chen, *ACS Energy Lett.*, 2020, **5**, 1665–1675.
67 M. Wu, G. Zhang, H. Yang, X. Liu, M. Dubois, M. A. Gauthier and S. Sun, *InfoMat*, 2022, **4**, e12265.
68 X. Zeng, J. Hao, Z. Wang, J. Mao and Z. Guo, *Energy Storage Mater.*, 2019, **20**, 410–437.
69 Y. Tian, Y. An, C. Wei, B. Xi, S. Xiong, J. Feng and Y. Qian, *Adv. Energy Mater.*, 2020, **11**, 2002529.
70 J. Peng, C. Zu and H. Li, *Energy Storage Sci. Technol.*, 2013, **2**, 55.
71 H. Li, *Joule*, 2019, **3**, 911.
72 H. Budde-Meiwes, J. Drillkens, B. Lunz, J. Muennix, S. Rothgang, J. Kowal and D. U. Sauer, *Proc. Inst. Mech. Eng., Part D*, 2013, **227**, 761.
73 Y. Wu, L. Xie, H. Ming, Y. Guo, J.-Y. Hwang, W. Wang, X. He, L. Wang, H. N. Alshareef, Y. K. Sun and J. Ming, *ACS Energy Lett.*, 2020, **5**, 807–816.
74 Y. Jin, L. Zou, L. Liu, M. H. Engelhard, R. L. Patel, Z. Nie, K. S. Han, Y. Shao, C. Wang, J. Zhu, H. Pan and J. Liu, *Adv. Mater.*, 2019, **31**, e1900567.
75 H. Pan, Y. Shao, P. Yan, Y. Cheng, K. S. Han, Z. Nie, C. Wang, J. Yang, X. Li, P. Bhattacharya, K. T. Mueller and J. Liu, *Nat. Energy*, 2016, **1**, 16039.
76 H. Luo, B. Wang, F. Wang, J. Yang, F. Wu, Y. Ning, Y. Zhou, D. Wang, H. Liu and S. Dou, *ACS Nano*, 2020, **14**, 7328–7337.
77 P. He, M. Yan, X. Liao, Y. Luo, L. Mai and C.-W. Nan, *Energy Storage Mater.*, 2020, **29**, 113–120.
78 G. G. Yadav, D. Turney, J. Huang, X. Wei and S. Banerjee, *ACS Energy Lett.*, 2019, **4**, 2144–2146.
79 G. G. Yadav, J. W. Gallaway, D. E. Turney, M. Nyce, J. Huang, X. Wei and S. Banerjee, *Nat. Commun.*, 2017, **8**, 14424.
80 X. Zeng, J. Liu, J. Mao, J. Hao, Z. Wang, S. Zhou, C. D. Ling and Z. Guo, *Adv. Energy Mater.*, 2020, **10**, 1904163.
81 J. Lei, Y. Yao, Z. Wang and Y. C. Lu, *Energy Environ. Sci.*, 2021, **14**, 4418–4426.